J. Fluid Mech. (1989), *vol.* 204, *pp.* 389–404
Printed in Great Britain

Evolution and decay of cylindrical and spherical nonlinear acoustic waves generated by a sinusoidal source

By P. L. SACHDEV AND K. R. C. NAIR
Department of Applied Mathematics, Indian Institute of Science, Bangalore-560012, India

(Received 12 July 1988 and in revised form 8 December 1988)

The present work gives a comprehensive numerical study of the evolution and decay of cylindrical and spherical nonlinear acoustic waves generated by a sinusoidal source. Using pseudospectral and predictor–corrector implicit finite difference methods, we first reproduced the known analytic results of the plane harmonic problem to a high degree of accuracy. The non-planar harmonic problems, for which the amplitude decay is faster than that for the planar case, are then treated. The results are correlated with the known asymptotic results of Scott (1981) and Enflo (1985). The constant in the old-age formula for the cylindrical canonical problem is found to be 1.85 which is rather close to 2, 'estimated' analytically by Enflo. The old-age solutions exhibiting strict symmetry about the maximum are recovered; these provide an excellent analytic check on the numerical solutions. The evolution of the waves for different source geometries is depicted graphically.

1. Introduction

The nonlinear acoustic waves generated by a sinusoidal source are described by the generalized Burgers equation

$$U_r - [(\gamma+1)/2a_0^2]\, UU_\tau + JU/2r = (\Delta/2a_0^3)\, U_{\tau\tau}, \tag{1.1}$$

where U is the particle velocity, τ is the retarded time $t - r/a_0$, a_0 is the small-signal sound speed, Δ is the diffusivity of sound (Lighthill 1956), γ is the adiabatic exponent, and $J = 1$ or 2 for cylindrical or spherical waves, respectively. The derivation of these equations may be found in Leibovich & Seebass (1974) and Sachdev (1987). The boundary condition on the source $r = r_0$ is

$$U(r_0, \tau) = U_0 \sin(\omega\tau), \tag{1.2}$$

where U_0 is the amplitude and ω the frequency of the sinusoidal source. The boundary condition (1.2) ignores the particular nonlinear effect associated with finite displacement of the piston, it being purely local and of no significance away from the piston.

The problem (1.1)–(1.2) is rendered non-dimensional by the transformation

$$V = (r/r_0)^{\frac{1}{2}J}\, U/U_0, \quad \theta = \omega\tau, \tag{1.3}$$

$$R_0 = (\gamma+1)\, U_0 \omega r_0/2a_0^2, \tag{1.4a}$$

$$\epsilon = \omega\Delta/(\gamma+1)\, U_0 R_0 a_0, \quad R = 2R_0\{(r/r_0)^{\frac{1}{2}} - 1\} \quad \text{for } J = 1, \tag{1.4b}$$

$$\epsilon = \omega\Delta/(\gamma+1)\, U_0 a_0, \quad R = R_0 \ln(r/r_0) \quad \text{for } J = 2, \tag{1.4c}$$

so that for the cylindrical case, the problem (1.1)–(1.2) becomes

$$V_R - VV_\theta = \epsilon[\tfrac{1}{2}R + R_0]\, V_{\theta\theta}, \tag{1.5}$$

$$V(0,\theta) = \sin(\theta) \quad (0 \leqslant \theta \leqslant \pi), \tag{1.6}$$

while for the spherical case, $J = 2$, it becomes

$$V_R - VV_\theta = \epsilon \exp(R/R_0)\, V_{\theta\theta}, \tag{1.7}$$

and (1.6). Since (1.1) preserves the parity and periodicity of the boundary value, we take only the principal interval $0 \leqslant \theta \leqslant \pi$, and impose the boundary end conditions

$$V(R,0) = V(R,\pi) = 0. \tag{1.8}$$

The (nonlinear) harmonic problem for the plane symmetry is described by the standard Burgers equation

$$V_R - VV_\theta = \epsilon V_{\theta\theta}, \tag{1.9}$$

together with the boundary conditions (1.6) and (1.8). This problem in its initial-value formulation, where R and θ are replaced by t and x, respectively, and V is changed to $-V$, has been treated in a fairly exhaustive way by Cole (1951). Indeed, it has a rich history with contributions from several other investigators (Fubini 1935; Fay 1931; Blackstock 1964; see Sachdev 1987). The analytic treatment of the plane harmonic problem became possible owing to access to Hopf–Cole transformation which changes (1.9) to the heat equation with a correspondingly simple transformation of the boundary (initial) condition (1.6). This problem was also treated by matched asymptotic expansion by Lesser & Crighton (1975), and Parker (1980). These studies threw further light on the structure of the solution, particularly in the early stages of the evolution of the profile when the shock is relatively thin and its structure is essentially Taylor-type with a simple balance between nonlinear convection and small (linear) diffusion. It is pertinent to briefly delineate the evolution of the sine wave as governed by (1.9) during the entire course of the wave propagation. First, when the profile $V = \sin(\theta)$ distorts owing to nonlinear convection alone ($\epsilon = 0$ in (1.8)), the solution is described by the implicit form

$$V = \sin(p), \quad p = \theta + R\sin(p), \tag{1.10}$$

which has an explicit Fourier series representation

$$V = 2\sum_{n=1}^{\infty}\left(\frac{J_n(nR)}{nR}\right)\sin(n\theta), \tag{1.11}$$

(Fubini 1935), where J_n is a Bessel function of order n. As the profile steepens on its front, it breaks, assuming a multiple-valued character. It then evolves under the Burgers equation (1.9) and experiences its embryonic stage. After a short duration it assumes a form with a balanced Taylor shock and is described by the composite solution

$$V = \left(\frac{1}{R+1}\right)\left(\frac{\pi\tanh\pi\theta}{2\epsilon(R+1)} - \theta\right), \tag{1.12}$$

with a tanh form of the shock. The profile gradually transforms itself and is then described by

$$V = 2\epsilon\sum_{n=1}^{\infty}\frac{\sin(n\theta)}{\sinh[n\epsilon(R+1)]}. \tag{1.13}$$

The solutions (1.12) and (1.13) overlap over large R values. The solution (1.13) is referred to as the Fay solution. It is the Fourier series version of the composite solution made up of the sawtooth solution

$$V \sim \frac{\pi-\theta}{R+1}, \tag{1.14}$$

and the shock solution

$$V(R,\theta) = h(R)\tanh[\tfrac{1}{2}h(R)\,\theta/\epsilon], \quad h(R) = (1/R)\,J_0^{-1}(1/R). \tag{1.15}$$

Here $J_0(x) = \sin(x)/x$ is the spherical Bessel function and J_0^{-1} is the function inverse to J_0. The solution (1.13) displays clearly the generation of higher harmonics during the distortion of the wave due to nonlinearity. The asymptotic 'old-age' form is

$$V = 4\epsilon\exp(-\epsilon R)\sin(\theta). \tag{1.16}$$

This form of the solution reflects two features: the reduced amplitude of the first harmonic in its old age and the non-appearance of any parameter describing the initial amplitude. (The parameter ϵ can be scaled out of (1.9) and (1.16).) The latter phenomenon is called amplitude saturation. We may point out the interesting fact that Cole (1951) in his basic paper had derived the formulae (1.10)–(1.13) from the solution of the initial-value problem (1.9) and (1.6) as approximations under certain limiting processes. These were subsequently shown to be exact solutions of the problem holding in different regimes. Besides, Lesser & Crighton (1975) and Parker (1980) derived the (exact) solution (1.13) as the first-order matched asymptotic solution of the same problem. Thus this matched asymptotic (expansion) first-order solution turns out to be an exact solution! We may close the review of the plane case by the comment that the transitions from one form of the solution of (1.9) to another are not clearly delineated and need further elucidation, possibly by a numerical study.

The cylindrical and spherical problems (1.5) and (1.7) with the initial and boundary conditions (1.6) and (1.8) lose the facility of Cole–Hopf transformation (or one like it) and therefore their analysis is more difficult. An exact analytic solution does not seem feasible; one must seek either asymptotic solutions or precise numerical solutions which may verify the former and pave the way for further analysis. Before we discuss our numerical results, we summarize two asymptotic studies. The first is due to Scott (1981) which gives a thorough account of different cases that arise in the $(\epsilon-R_0)$-plane, for which some asymptotic solutions may be found. Here ϵ and R_0 are the two dimensionless parameters which appear in (1.5) and (1.7). The second study, due to Enflo (1985), attempts a solution for the cylindrical Burgers equation similar to the Fay solution for the plane one (see (1.13)). Since these studies have an important bearing on our results, we give them in some detail.

1.1. *A review of Scott's analysis*

The main object of Scott's paper was to set up expansions uniformly valid in ϵ and R_0 for the problems (1.5) and (1.7), with the conditions (1.6) and (1.8). This required the introduction of a number of matching asymptotic domains in the $(\epsilon-R_0)$-plane. Corresponding to each domain, various asymptotic regions in space–time were specified. Scott could give explicit asymptotic solutions in some of the domains in the $(\epsilon-R_0)$-plane for some regions in the $(\theta-R)$-plane. This became possible in cases where the governing asymptotic partial differential equation was either linear or the

standard Burgers equation or the inviscid equation. These were referred to as reducible problems. In some cases the problem proved to be irreducible in the sense that it required the solution of the full non-planar equation (1.5) or (1.7). In the cylindrical symmetry, the irreducible problem had the advantage that it had no parameter appearing in it; it was therefore referred to as canonical. It is this canonical problem that Enflo (1985) attempted to solve with a view to studying the saturation phenomenon, namely the amplitude of the final old-age wave turning out to be independent of the amplitude of the wave at the source. We list below all domains considered by Scott and summarize his analytic results for some representative cases in §3. For these cases we have definite corroboration with our numerical results. The domains in the cylindrical symmetry are denoted by C 1, C 2, ... and those of the spherical case by S 1, S 2, ...

(i) Cylindrical case

(C 1)	$\epsilon \ll 1$,	$\epsilon R_0^2 \ll 1$,	(C 2)	$\epsilon \ll 1$,	$\epsilon R_0^2 = O(1)$,
(C 3)	$\epsilon R_0 \ll 1$,	$\epsilon R_0^2 \gg 1$,	(C 4)	$\epsilon R_0^2 \gg 1$,	$\epsilon R_0 = O(1)$,
(C 5)	$\epsilon R_0 \gg 1$,	$\epsilon R_0^2 \gg 1$,	(C 6)	$\epsilon \gg 1$,	$\epsilon R_0^2 = O(1)$,
(C 7)	$\epsilon \gg 1$,	$\epsilon R_0^2 \ll 1$,	(C 8)	$\epsilon = O(1)$,	$R_0 \ll 1$.

(ii) Spherical case

(S 1)	$\epsilon \exp(1/R_0)/R_0^2 \gg 1$,	$\epsilon R_0 \ll 1$,	(S 2)	$\epsilon \exp(1/R_0)/R_0^2 = O(1)$,	$\epsilon R_0 \ll 1$,
(S 3)	$\epsilon \exp(1/R_0)/R_0^2 \ll 1$,	$\epsilon R_0 \ll 1$,	(S 4)	$\epsilon R_0 = O(1)$,	$\epsilon \ll 1$,
(S 5)	$\epsilon R_0 \gg 1$,	$\epsilon \ll 1$,	(S 6)	$R_0 \gg 1$,	$\epsilon = O(1)$,
(S 7)	$\epsilon R_0 \gg 1$,	$\epsilon \gg 1$,	(S 8)	$\epsilon R_0 = O(1)$,	$\epsilon \gg 1$.

1.2. *Comments on Enflo's work*

Enflo (1985) undertook to solve for cylindrical symmetry one of the irreducible problems of Scott (see (C 1) above), namely

$$U_x - UU_\theta = (\tfrac{1}{2}x)\, U_{\theta\theta}, \tag{1.17}$$

subject to the matching conditions

$$U = (1/x)[\pi \tanh(\pi\theta/x^2) - \theta] \quad (-\pi < \theta < \pi), \quad \text{as } x \to 0, \tag{1.18}$$

and

$$U = C \exp(-\tfrac{1}{4}x^2) \sin(\theta) \quad \text{as } x \to \infty. \tag{1.19}$$

He first recovered the Fay solution to the plane Burgers equation (see Appendix A of his paper)

$$U_x - UU_\theta = U_{\theta\theta}, \tag{1.20}$$

subject to the matching conditions

$$U = (1/x)[\pi \tanh(\pi\theta/2x) - \theta] \quad (-\pi < \theta < \pi), \quad \text{as } x \to 0, \tag{1.21}$$

and

$$U = C \exp(-x) \sin(\theta), \quad \text{as } x \to \infty, \tag{1.22}$$

similar to (1.18) and (1.19) (ϵ has been scaled out of the equation), by the ansatz

$$U(x, \theta) = C \sum_{n=1}^{\infty} \exp(-nx) f_n(\theta). \tag{1.23}$$

This was essentially the approach adopted by Fay himself. By substituting (1.23) into (1.20) and equating coefficients of powers of $\exp(-nx)$ to zero, Enflo obtained an infinite system of linear ordinary differential equations for the functions $f_n(\theta)$,

which he solved recursively. The unknown constants which appear in the solution were chosen 'judiciously' to recover the form of the Fay solution. In particular, the matching of the solution (1.23) at $x \sim 0$, for small x such that $nx = O(1)$, and $\theta \ll x$ with the solution (1.21) led to the exact determination of the old-age constant. It must be emphasized that the knowledge of the exact Fay solution was a considerable help in this analysis. We may here compare our asymptotic treatment of cylindrical N waves (see Sachdev, Tikekar & Nair 1986) with Enflo's work. Introducing several transformations motivated by the knowledge of the plane N wave, we could find an exact asymptotic solution of the cylindrical N wave, leading to an exact analytic form for the Reynolds number which involved two unknown arbitrary constants. In our case, the independent variables in the expansion corresponding to (1.23) were time and the similarity variable. We also made use of the (asymptotic) inviscid solution near the node $x = 0$ and the old-age form of the N wave to derive the form of the fully nonlinear N wave regime. However, this approach failed to provide an analytic asymptotic result for the spherical N wave.

Enflo sought the asymptotic solution of the problem (1.17)–(1.19) in the form

$$U(x, \theta) = C \sum_{n=1}^{\infty} \exp(-\tfrac{1}{4}nx^2) f_n(x, \theta), \tag{1.24}$$

with the choice $f_1(\theta) = \sin(\theta)$. He was again able to write the solution of the functions f_n recursively in the form

$$f_1 = C_{11} \sin(\theta), \quad C_{11} = 1,$$

$$f_2 = C_{22}(x) \sin(2\theta),$$

$$f_3 = C_{33}(x) \sin(3\theta) + C_{31}(x) \sin(\theta),$$

$$\vdots$$

$$f_n = C_{nn}(x) \sin(n\theta) + C_{n,n-2}(x) \sin[(n-2)\theta] + \ldots + \begin{cases} C_{n1}(x) \sin(\theta), & n \text{ odd}, \\ C_{n2}(x) \sin(2\theta), & n \text{ even}. \end{cases}$$

The functions C_{11}, C_{22}, C_{33} and C_{44} could be explicitly determined. The general form for C_{nk} was written out but was found to be too involved for explicit determination. Enflo, therefore, attempted an asymptotic evaluation of the functions C_{nr} for $r^2 \neq n$. He sought the behaviour of C_{kk} in the form

$$C_{kk} \approx (\tfrac{1}{2}C)^{k-1} x \exp[k(\alpha + \beta x^2)].$$

To determine the constants α and β Enflo resorted to some kind of 'curve fitting' and extrapolation. We omit the details here. It is remarkable that by this approximate approach he arrived at a value fairly close to the constant C in the old-age solution, as we shall demonstrate in §3 where we give the numerical results of the present problem. We surmise that the expansion of (1.17) in an infinite series in x and θ is probably much more complicated than that for (1.20). This approach due to Enflo is very interesting but would require further careful pursuing.

2. Plane nonlinear harmonic waves

It is useful first to study the solution of the plane Burgers equation (1.9), subject to the sinusoidal initial and boundary conditions (1.6) and (1.8). This study serves several purposes; (i) while the solution of the problem is known due to Cole–Hopf transformation (Cole 1951), it has different forms in different R (time-like) regions; each of these solutions is exact. One must be able to visualize clearly the transitions

and duration of the different solution regimes; (ii) proper understanding of these should aid the search for analytic solutions for the non-planar Burgers equation and (iii) the numerical methods employed for non-planar Burgers equations can be checked for their stability, accuracy and computational economy. We may point out that the numerical simulation of the initial boundary-value problem (1.9), (1.6) and (1.8) is by no means a trivial task as will become evident from the following.

From physical arguments concerning the build-up of the waves from the signals at the source, it is not difficult to convince oneself that in the earliest stage of the wave evolution, the propagation is essentially inviscid so that (1.9) is replaced by

$$V_R - VV_\theta = 0. \tag{2.1}$$

This equation with the initial and boundary conditions (1.6) and (1.8), respectively, has the implicit solution (1.10). This solution was written in terms of the Fourier sine series by Fubini (see (1.11)), with Fourier coefficients involving Bessel functions. The solution (1.10) or (1.11) remains single valued until $R = 1$ when it breaks to become multiple valued near $\theta = 0$. Away from $\theta = 0$ the solution (1.10) is still valid. At $R = 1$, one must introduce a small viscous term to balance the nonlinear convective term to obtain a smooth shock transition. Thus, (1.9) now takes over. It was shown by Lesser & Crighton (1975), and later by Parker (1980), using a singular perturbation argument that the first-order matched asymptotic solution of (1.9) and (1.6) is the composite solution (1.12). It is remarkable that this matched asymptotic solution is in fact exact. However, between the inviscid solution (1.10) and the composite solution (1.12), there is a small region $R = O(1)$ over which the inviscid solution (1.10) adjusts itself to the composite solution (1.12). This is called the embryonic shock region. The solution of (1.9) evolves further, the thin shock broadens, the hypotheses on which the singular perturbation solution was derived fail. Thus, for $R = O(\epsilon^{-1})$, the composite solution breaks down. Fortunately, there is a Fourier series version (1.13) of the composite solution (1.12) (see Lesser & Crighton 1975) which begins to operate well before the composite solution fails. This solution holds all the way until the wave has died out sufficiently and viscosity has become significant everywhere and not just in the narrow-shock region. The solution then has entered its old age and is governed by the first term in the series (1.13), namely (1.16).

Thus, for $R \gg \epsilon^{-1}$, the wave contains only a single Fourier component which decays under viscosity alone. The constant 4 in the old-age solution (1.16) is the universal constant for this plane canonical problem for all ϵ. (Indeed, the parameter ϵ can be scaled out of (1.9).)

Now, we turn to the numerical validation and elucidation of the above analytic results.† First, we solved (1.9) with initial and boundary conditions (1.6) and (1.8) using a pseudospectral scheme. The finite-difference analogue of this scheme for the problem

$$V_R - VV_\theta = \epsilon g(R)\, V_{\theta\theta}, \tag{2.2}$$

with $g(R) = 1$, $\frac{1}{2}R + R_0$, and $\exp(R/R_0)$ for plane, cylindrical and spherical Burgers equation, respectively, is

$$V(R+\Delta R, \theta) = V(R,\theta) + \Delta R V_R + (1/2!)\,\Delta R^2 V_{RR} + \ldots, \tag{2.3}$$

† The details of numerical results reported in this paper may be obtained directly from the authors or the Editor.

where V_R, V_{RR} and V_{RRR} are obtained from (2.2) and its derivatives with respect to R. Thus,

$$V_R = VV_\theta + \epsilon g(R)\, V_{\theta\theta}, \tag{2.4}$$

$$V_{RR} = V_R\, V_\theta + VV_{R\theta} + \epsilon g(R)\, V_{R\theta\theta} + \epsilon g'(R)\, V_{\theta\theta}, \tag{2.5}$$

$$V_{RRR} = V_{RR}\, V_\theta + 2V_R\, V_{R\theta} + VV_{RR\theta} + \epsilon g(R)\, V_{RR\theta\theta} + 2\epsilon g'(R)\, V_{R\theta\theta} + \epsilon g''(R)\, V_{\theta\theta}. \tag{2.6}$$

The derivatives of V, V_R, V_{RR}, etc. with respect to θ are evaluated using a truncated Fourier series. The finite Fourier transform of $V(R,\theta)$ is defined as

$$\bar{V}(R,k_j) = (1/K) \sum_{p=0}^{K-1} V(R, p\Delta\theta) \exp(-\mathrm{i}k_j p\Delta\theta), \tag{2.7}$$

over the scaled interval $(0, 2\pi)$ of θ. Here, $\theta = 2\pi/K$, K denoting the number of mesh points and k_j are the wavenumbers varying between 0 and $K-1$. The inverse Fourier transform is

$$V(R, p\Delta\theta) = \sum_{|k_j|<\frac{1}{2}K} \bar{V}(R,k_j) \exp(\mathrm{i}k_j p\Delta\theta). \tag{2.8}$$

The spatial derivatives at the mesh points are

$$V_\theta(R, p\Delta\theta) = \sum_{|k_j|<\frac{1}{2}K} (\mathrm{i}k_j)\, \bar{V}(R,k_j) \exp(\mathrm{i}k_j p\Delta\theta), \tag{2.9}$$

$$V_{\theta\theta}(R, p\Delta\theta) = \sum_{|k_j|<\frac{1}{2}K} (\mathrm{i}k_j)^2\, \bar{V}(R,k_j) \exp(\mathrm{i}k_j p\Delta\theta), \tag{2.10}$$

etc. The solution at $R+\Delta R$ is accurate to $O[(\Delta R)^4]$. The numerical solution manifests small oscillations near $\theta = 0$ for $R > 1$, if we choose the domain to be $0 \leqslant \theta \leqslant \pi$. The use of the profile over the full period $-\pi < \theta < \pi$ obviates this difficulty and the solution proceeds smoothly. The analytic solution in the Fubini series (1.11) does not converge near $\theta = 0$. We therefore, used the implicit solution (1.10) and evaluated it numerically using the Newton–Raphson method. The numerical and analytic solutions agree very well (see table 1). Figure 1 shows the evolution of the profile from $R = 0$ to $R = 10$. For $R > 1$, the profile transforms to acquire a balanced Taylor shock passing through the embryonic shock regime. Figure 1 also gives a total view of the evolution of the sine curve through all its forms – inviscid, sharp shock, evolutionary shock and thick shock stage. While the initial sine wave evolves under the influence of the plane Burgers equation its peak moves to the left, up to $R \approx 2$, and then to the right. The peak establishes itself at the middle of the half wave, $\theta = \frac{1}{2}\pi$, with the onset of the old age at $R \approx 500$. It continues to be so until the profile completely vanishes. When $R \approx 5$, the profile becomes smooth enough to warrant a switch to the predictor–corrector implicit finite-difference scheme which is several times faster than the pseudospectral scheme (see Sachdev *et al.* 1986). The implicit finite-difference analogue of equation (2.2) is as follows:

Predictor:

$$V_{i+1,j+\frac{1}{2}} - 2[1 + h^2/(\epsilon k g_{j+\frac{1}{2}})]\, V_{i,j+\frac{1}{2}} + V_{i-1,j+\frac{1}{2}} = -[h/(2\epsilon g_{j+\frac{1}{2}})]\, V_{i,j}[4h/k][V_{i+1,j} - V_{i-1,j}], \tag{2.11}$$

	$V(R=0.1,\theta)$		$V(R=0.5,\theta)$		$V(R=1,\theta)$	
θ	Numerical	Fubini	Numerical	Fubini	Numerical	Fubini
0.0000	0.0000	0.0000	0.0000	0.0000	0.0000	0.0000
0.0614	0.0682	0.0682	0.1200	0.1221	0.5236	0.6616
0.1227	0.1359	0.1360	0.2363	0.2407	0.7321	0.7930
0.1841	0.2029	0.2032	0.3466	0.3527	0.8316	0.8689
0.2454	0.2689	0.2693	0.4486	0.4559	0.8915	0.9183
0.5522	0.5723	0.5730	0.8127	0.8207	0.9892	0.9998
0.8590	0.8070	0.8079	0.9688	0.9750	0.9612	0.9675
1.1658	0.9517	0.9527	0.9911	0.9957	0.8822	0.8864
1.4726	0.9990	1.0000	0.9296	0.9329	0.7749	0.7778
1.7794	0.9530	0.9539	0.8134	0.8159	0.6499	0.6520
2.0862	0.8252	0.8260	0.6607	0.6625	0.5132	0.5147
2.3930	0.6319	0.6324	0.4837	0.4848	0.3688	0.3698
2.6998	0.3912	0.3915	0.2910	0.2917	0.2194	0.2200
3.0066	0.1222	0.1223	0.0897	0.0899	0.0673	0.0675
3.0680	0.0668	0.0668	0.0490	0.0491	0.0367	0.0368
3.1293	0.0111	0.0111	0.0082	0.0082	0.0061	0.0061
3.1416	0.0000	0.0000	0.0000	0.0000	0.0000	0.0000

Note: 'Numerical, analytic, Fubini, sawtooth, composite and Fay' in Tables 1–4 (see solutions (1.10)–(1.14)).

TABLE 1. Numerical and analytic (Fubini (1.10)) solutions of the Burgers equation (1.9)

Corrector:

$$[1+\{h/(2\epsilon g_{j+\frac{1}{2}})\}\,V_{i,j+\frac{1}{2}}]\,V_{i+1,j+1}-2[1+h^2/(\epsilon g_{j+\frac{1}{2}})]\,V_{i,j+1}+[1-\{h/(2\epsilon g_{j+\frac{1}{2}})\}\,V_{i,j+\frac{1}{2}}]\,V_{i-1,j+1}$$
$$=-[1+\{h/(2\epsilon g_{j+\frac{1}{2}})\}\,V_{i,j+\frac{1}{2}}]\,V_{i+1,j}+2[1-h^2/(k\epsilon g_{j+\frac{1}{2}})]\,V_{i,j}$$
$$-[1-\{h/(2\epsilon g_{j+\frac{1}{2}})\}\,V_{i,j+\frac{1}{2}}]\,V_{i-1,j}. \tag{2.12}$$

Here, $V(R,\theta)=V(R_j,\theta_i)=V_{i,j}$, $R_j=j\Delta R$ and $\theta_i=\mathrm{i}\Delta\theta$. The mesh sizes are $h=\Delta\theta=\pi/M$, and $k=\Delta R=1/N$, where M and N are the number of mesh points in the θ and R ranges, respectively. $j=0$ corresponds to $R=0$, and $i=0$ and M correspond to $\theta=0$ and $\theta=\pi$, respectively. Thus, at the boundaries, $V_{i,0}=\sin(\theta_i)$, $i=0,1,\ldots,M$ and $V_{0,j}=V_{M,j}=0$ for $j=0,1,2,\ldots$. Equation (2.11) is linear in $V_{k,j+\frac{1}{2}}$, $k=i-1$, i and $i+1$. Since the associated coefficient matrix in the solution is invariant throughout the computation, it is enough to invert it just once. Equation (2.3) is nonlinear in $V_{k,j+1}$, $k=i-1$, i and $i+1$. The associated coefficient matrix in the solution depends on the predicted values at $R_{j+\frac{1}{2}}$. It has to be inverted at each computing level R_{j+1}.

Douglas & Jones (1963) demonstrated the convergence of scheme (2.11)–(2.12) for the nonlinear PDEs of the parabolic class including the equations of the Burgers type. The truncation error of the scheme is $O(h^2+k^2)$. For profiles without discontinuities and with smooth gradients, the scheme (2.11)–(2.12) delivers very good solutions. For $R\gg 1$, the numerical solution agrees very closely with the analytic solution (composite and Fay) wherever the latter are valid (see table 2). Both the solutions (composite and Fay) hold for a fairly long duration. The former begins to fail when $R\approx 200$, but the latter continues to furnish very good results all the way to the extinction of the profile. It is interesting to note that soon after the

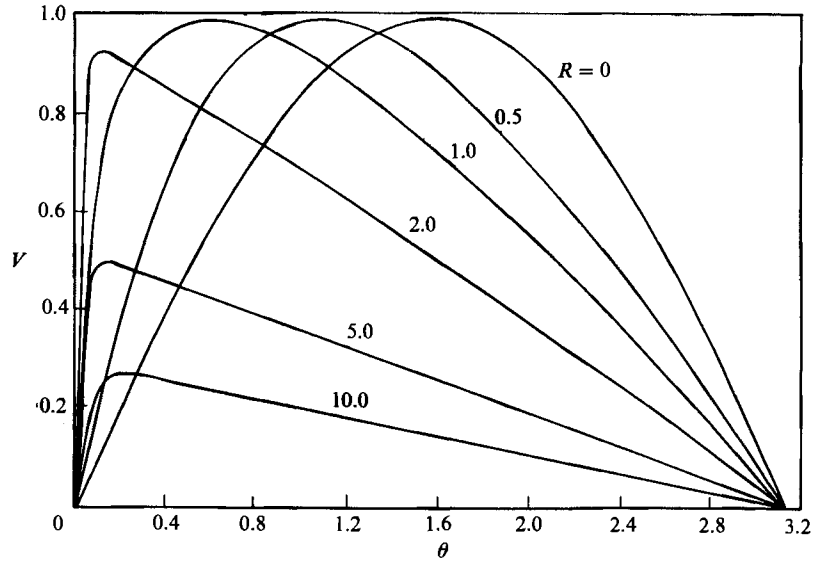

FIGURE 1. Numerical solution of the Burgers equation (1.9) at $R = 0.5$, 1, 2, 5, and 10 (initial profile at $R = 0$ is also shown).

	$V(R = 100, \theta)$			$V(R = 200, \theta)$		
θ	Numerical	Composite	Fubini	Numerical	Composite	Fubini
0.0000	0.0000	0.0000	0.0000	0.0000	0.0000	0.0000
0.0614	0.0024	0.0024	0.0024	0.0005	0.0004	0.0004
0.1227	0.0047	0.0047	0.0047	0.0009	0.0009	0.0009
0.1841	0.0069	0.0068	0.0068	0.0013	0.0013	0.0013
0.2454	0.0089	0.0089	0.0089	0.0018	0.0017	0.0017
0.5522	0.0162	0.0162	0.0162	0.0036	0.0036	0.0036
0.8590	0.0186	0.0186	0.0186	0.0049	0.0049	0.0049
1.1658	0.0180	0.0179	0.0179	0.0055	0.0055	0.0055
1.4726	0.0159	0.0159	0.0159	0.0055	0.0055	0.0055
1.7794	0.0132	0.0132	0.0132	0.0050	0.0050	0.0050
2.0862	0.0104	0.0104	0.0104	0.0041	0.0041	0.0041
2.3930	0.0074	0.0074	0.0074	0.0031	0.0030	0.0031
2.6998	0.0044	0.0044	0.0044	0.0019	0.0017	0.0019
3.0066	0.0013	0.0013	0.0013	0.0006	0.0004	0.0006
3.1293	0.0001	0.0001	0.0001	0.0001	*	0.0001
3.1416	0.0000	0.0000	0.0000	0.0000	*	0.0000

* Composite solution is not valid.

TABLE 2. Numerical and analytic (composite (1.12) and Fay (1.13)) solutions of the Burgers equation (1.9)

old age sets in, the profile becomes symmetric again about $\theta = \frac{1}{2}\pi$ and continues to be so until it is nearly extinct at $R \approx 1000$. The profile, becoming symmetric once again, is a good indication of the onset of old age. The old-age solution provided an excellent check on the numerical solution. The constant C in the old-age solution is recovered as 3.99, in close agreement with its analytic value equal to 4.

We briefly give the domains of validity of the various analytic solutions – Fubini,

sawtooth, composite and Fay. For $R < 1$, the Fubini solution (1.10) holds good for $0 \leqslant \theta \leqslant \pi$. It ceases to hold for $R \geqslant 1$, near $\theta = 0$ but is still valid for $\theta \gg 0$. Here, even the sawtooth solution holds well away from $\theta = 0$. For $R \leqslant 3$, the sawtooth solution continues to hold for $\theta > 0$. For $R > 3$ the composite solution takes over and holds everywhere in $0 \leqslant \theta \leqslant \pi$. The sawtooth solution begins to fail for all θ when $R > 5$ while the composite and Fay solutions provide good results. This is so until $R \approx 200$ when the former fails while the latter continues to provide excellent results. It may be noted that the Fay solution agrees with the numerical solution to more than four decimal places over a long range spanning between $R \approx 5$ and $R \approx 900$. For $R > 500$ the old-age analytic solution provides excellent results. In several overlapping regimes, even though the solutions do not hold near $\theta = 0$, they give excellent results elsewhere (with an accuracy of about four decimal places). For example, the Fubini and composite solutions agree very well with the numerical solution for $0 \ll \theta < \pi$ when $R > 1$.

Equation (1.9) was also solved with the initial profile at $R = 1$ (see (1.10)). This profile has a sharp shock near $\theta = 0$. We used the pseudospectral scheme until the shock smoothed out. The predictor–corrector scheme was then used for fast computation. The numerical value of the old-age constant C in this case is also found to be 4.

3. Spherical and cylindrical harmonic waves – numerical results and comparison with asymptotic results

Since there is no Hopf–Cole transformation for spherical and cylindrical Burgers equations, an explicit solution for the harmonic problem for these cases is not feasible. There are asymptotic results of Crighton & Scott (1979) and Scott (1981) which provide analytic forms in some parametric domains and prove helpful in the numerical study of the non-planar problems. As we have noted in §1, Scott's asymptotic study in the $(\epsilon - R_0)$-plane leads to four important categories of reduced problems and their solutions. We have therefore found it convenient to carry out our numerical studies for choices of parameters ϵ and R_0, which are typical of each of these categories, for both spherical and cylindrical geometries.

(i) The asymptotic expansion leads to a canonical problem with no parameter appearing explicitly in it. In the cylindrical case, the canonical problem may be stated as follows:

$$F_s - FF_\theta = \tfrac{1}{2} sF_{\theta\theta}, \tag{3.1a}$$

$$sF \sim \pi \tanh\left(\pi\theta/s^2\right) - \theta] \quad \text{as } s \to 0, \tag{3.1b}$$

$$F \sim C \exp\left(-\tfrac{1}{4}s^2\right) \sin\theta \quad \text{as } s \to \infty. \tag{3.1c}$$

This is the problem discussed by Enflo (1985). The old-age constant C is 'universal' in the sense that it does not depend on the parameters ϵ and R_0. This canonical case manifests the saturation phenomenon rather dramatically (see (v) below). We remark that Scott's analysis for the spherical Burgers equation does not lead to any canonical problem for it.

(ii) The asymptotic expansion results either in an irreducible form in which ϵ and R_0 or some combination of both appears . The specific parameters to represent this domain are chosen to be (*a*) $\epsilon = 1$ and $R_0 = 0.01$ for $J = 1$ and (*b*) $\epsilon = 0.05$ and

$R_0 = 20$ for $J = 2$ (see (C 8) and (S 4) in §1). The asymptotic old-age solution for the cylindrical symmetry is

$$V \sim C(\epsilon) \exp\left[-\epsilon\{\tfrac{1}{4}R^2 + R_0 R\}\right] \sin\theta \quad (R \gg 1). \tag{3.2}$$

The constant C for $\epsilon = 0.01$ was found to be 0.88. This constant was found to have the same value for another choice of the parameters, $\epsilon = 1$ and $R_0 = 0$ belonging to the same domain. The asymptotic solution of the spherical Burgers equation is

$$V \sim \tfrac{1}{2}\epsilon \frac{D(a)}{a} \exp\left(-ae^{R/R_0}\right) \sin\theta \quad (a = \epsilon R_0). \tag{3.3}$$

The constant $D(a)$ for $a = 1$ was found to be 29.5 numerically. This value of $D(a)$ agrees closely with that of Scott shown in his figure 3 (see Scott 1981, p. 221). The numerical and analytic (asymptotic) solutions of the cylindrical and spherical Burgers equations agree very closely (see Nair 1988).

(iii) The asymptotic expansion leads to the Burgers equation with one or more parameters appearing in it. The typical parametric choices are (*a*) $\epsilon = 0.01$ and $R_0 = 100$ for $J = 1$ and (*b*) $\epsilon = 0.05$ and $R_0 = 200$ for $J = 2$ [see (C 4) and (S 5) in §1]. The asymptotic form of solutions in these cases is

$$V \sim 4C\epsilon \exp\left[-\epsilon(\tfrac{1}{4}R^2 + R_0 R)\right] \sin\theta \quad (J = 1), \tag{3.4}$$

and

$$V \sim 4\epsilon \exp\left[a\{1 - \exp(R/R_0)\}\right] \sin\theta \quad (J = 2), \tag{3.5}$$

where $C = R_0 I_1[1/(2\epsilon R_0)]/I_0[1/(2\epsilon R_0)]$, I_n being the modified Bessel function of the first kind. There is again a good agreement between the asymptotic and numerical solutions.

(iv) This is the case in which a quick transition to linearized (old-age) form takes place so that various intermediate stages are swept over at $R = O(1)$. The typical values of the parameters are (*a*) $\epsilon = 0.1$ and $R_0 = 50$ for $J = 1$ and (*b*) $\epsilon = 5$ and $R_0 = 0.5$ for $J = 2$ (see C 5) and (S 7) in §1). We had to choose a mesh size $O(10^{-4})$ for R to overcome the initial numerical instability near $\theta = 0$. The asymptotic old-age solution for $J = 1$ is

$$V \sim \exp\left[-\epsilon\{\tfrac{1}{4}R^2 + R_0 R\}\right] \sin(\theta), \tag{3.6}$$

and that for $J = 2$ is

$$V \sim \exp\left[-a(\exp(R/R_0) - 1)\right] \sin(\theta) \quad (a = \epsilon R_0). \tag{3.7}$$

The asymptotic solutions (3.6)–(3.7) and the corresponding numerical solutions were found to be in good agreement (see Nair 1988).

(v) Amplitude saturation. Saturation is said to occur when the amplitude of the wave for large R becomes independent of the source amplitude. In the cylindrical symmetry, this happens for the domains (C 1), (C 2) and (C 3) (see §1). The (asymptotic) reduced problem is free of all parameters as we pointed out in §1. The saturation occurs naturally in the canonical problem (see (3.1)).

We solved numerically the problem (1.5) with initial and boundary conditions (1.6) and (1.8) with several sets of parameters and amplitudes: (i) $\epsilon = 0.01$, $R_0 = 1$, (ii) $\epsilon = 0.04, R_0 = 0.5$ and (iii) $\epsilon = 0.02, R_0 = 0.5$. For cases (i) and (ii) the initial profile is calculated at $R = 1$ from the inviscid solution while for case (iii) it is $V = \sin\theta$ at $R = 0$. The constant C in the numerical solution converges in the near old-age regime to 1.95, 1.85 and 1.85, respectively for cases (i), (ii) and (iii). We surmise that this

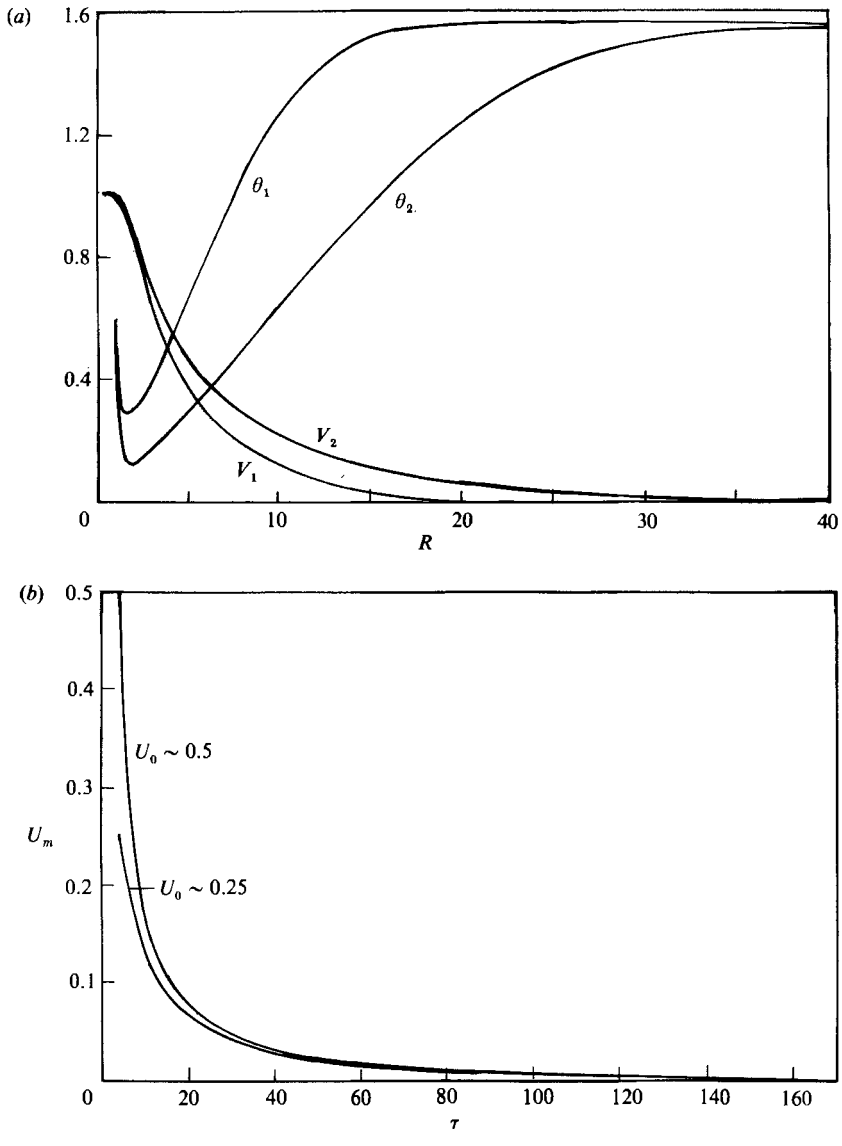

FIGURE 2. (*a*) Maximum value of the amplitude $V_{\max}$ and its position for the solution of (1.5) for (i) $\epsilon = 0.01$, $R_0 = 1$ and (ii) $\epsilon = 0.04$, $R_0 = 0.5$. (*b*) Maximum value of the amplitude U for (i) $U_0 = 0.5$ and (ii) $U_0 = 0.25$.

constant is about 1.85. It is very close to 2, the value 'estimated' by Enflo. The maximum amplitude of the profile at various R as given by the old-age formula

$$V \sim C\epsilon^{\frac{1}{2}} \exp -(\tfrac{1}{4}R^2 + R_0 R) \quad \sin\theta, \tag{3.8}$$

with $C = 1.85$ and that from the numerical solution agree very well. Here, as in the plane case, the re-emergence of the symmetry in the profile about $\theta = \frac{1}{2}\pi$ proves invaluable in demarcating the onset of old age. The latter solution provides an excellent check on the numerical solution. The amplitude in old age falls exponentially with the solution maintaining perfect symmetry about $\theta = \frac{1}{2}\pi$.

Figure 2(*a*) shows the amplitude $V_{\max}$ of the profiles in cases (i) and (ii) as they

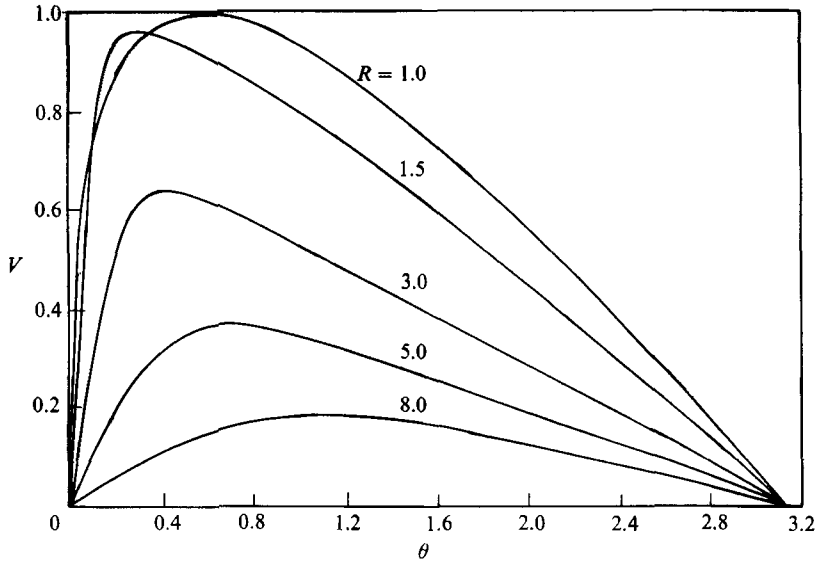

FIGURE 3. Solution of the cylindrical Burgers equation (1.5) at $R = 1$, 1.5, 3, 5 and 8.

evolve under the cylindrical Burgers equation (1.5). Figure 2(*b*) shows the corresponding amplitude in terms of the original variable U (see (1.3)–(1.4) for a relation between U and V). The amplitude of the initial profile in case (i) is double that in (ii). However, both the profiles diffuse to merge after, $r \sim 50$, and tend subsequently to their asymptotic behaviour (see (3.1)). This illustrates the phenomenon of saturation.

In the spherical symmetry the saturation takes place in the domains (S 4) and (S 5), and (S 6) under certain restrictions (see Scott 1981). The governing equation in the present case for the domain (S 4) is

$$F_s - FF_\theta = \exp(s/a) F_{\theta\theta}, \tag{3.9a}$$

where the parameter $a = \epsilon R_0$. The (asymptotic) matching condition is

$$sF \sim \pi \tanh(\pi\theta/2s) - \theta, \tag{3.9b}$$

as $s \to 0$, uniformly in $-\pi \leqslant \theta \leqslant \pi$.

We now discuss a sine wave as it evolves under a cylindrical or spherical Burgers equation (equations (1.5)–(1.8)). The evolutionary process covers the development of an embryo shock wave from the initial sine wave, its transformation into a Taylor shock and then into a thick shock and, finally, its decay in the old age (cf. Sachdev *et al.* (1986) for a similar study of the non-planar Burgers equation with discontinuous N wave initial condition). We also compare the numerical solution with the analytic (asymptotic) solutions (equation (3.11) below) of Scott. For this purpose, we choose the parameters to be $\epsilon = 0.04$ and $R_0 = 0.5$ for the cylindrical case, $J = 1$, which we treat first. Equation (1.5) was solved with the solution of (1.10) at $R = 1$ as the initial profile. This is the stage at which the sine wave has evolved into a sharp shock near $\theta = 0$ (see figure 3). In the next evolutionary stage, the embryo shock transforms into a quasi-steady shock, as depicted in figure 3. The latter assumes a Taylor structure when $R \approx 3$. The comparison of the numerical solutions in this regime with the (approximate) composite solution

$$V = [1/(R+1)][\pi \tanh \pi\theta/\epsilon(R+1)(R+2R_0) - \theta], \tag{3.10}$$

	$V(R=2,\theta)$		$V(R=5,\theta)$		$V(R=10,\theta)$	
θ	Numerical	Analytic	Numerical	Analytic	Numerical	Analytic
0.000	0.000	0.000	0.000	0.000	0.000	0.000
0.012	0.267	0.321	0.047	0.046	0.008	0.007
0.258	0.889	0.961	0.458	0.459	0.147	0.133
0.503	0.828	0.879	0.436	0.439	0.204	0.192
0.749	0.761	0.798	0.396	0.399	0.208	0.202
0.994	0.691	0.716	0.356	0.358	0.193	0.190
1.240	0.617	0.634	0.316	0.317	0.172	0.171
1.485	0.541	0.552	0.275	0.276	0.150	0.150
1.730	0.464	0.470	0.234	0.235	0.128	0.128
2.098	0.385	0.389	0.194	0.194	0.106	0.106
2.344	0.305	0.307	0.153	0.153	0.084	0.084
2.589	0.224	0.225	0.112	0.112	0.061	0.061
2.712	0.143	0.143	0.071	0.071	0.039	0.039

TABLE 3. Numerical and analytic [see equation (3.10)] solutions of the cylindrical Burgers equation [$\epsilon = 0.01$, $R_0 = 1$]

	Maximum value of V			Maximum value of V	
R	Numerical	Analytic	R	Numerical	Analytic
35.084	0.00622	0.00600	43.084	0.00122	0.00116
36.084	0.00516	0.00498	44.084	0.00097	0.00093
37.084	0.00427	0.00410	45.084	0.00077	0.00071
38.084	0.00351	0.00337	46.084	0.00061	0.00057
39.084	0.00287	0.00275	47.084	0.00048	0.00045
40.084	0.00233	0.00223	48.084	0.00038	0.00035
41.084	0.00189	0.00180	49.084	0.00029	0.00027
42.084	0.00152	0.00145	51.151	0.00017	0.00016

TABLE 4. Old-age (numerical and asymptotic) solutions of the cylindrical Burgers equation ($C = 1.85$, $\epsilon = 0.01$, $R_0 = 1$)

is shown in table 3. There is a reasonable agreement in $2 < R < 10$. This is followed by the shock thickening. When $R \simeq 12$, the wave shows a tendency to become symmetric about $\theta = \frac{1}{2}\pi$. It becomes essentially symmetric about $\theta = \frac{1}{2}\pi$ at $R = 20$ when the old-age regime sets in. At this stage the wave has sufficiently damped, the evolution is controlled purely by the linearized form of (1.5), and the nonlinear term hardly contributing in the competing processes. The old-age solution is shown in table 4. This table also shows the asymptotic solution

$$V = C\epsilon^{\frac{1}{3}} \exp -[\epsilon\{\tfrac{1}{4}R^2 + R_0 R\}] \sin\theta, \tag{3.11}$$

(see Scott 1981). The numerical solution and the asymptotic solution (3.11), with $C = 1.85$, agree very closely.

Now we discuss the sine wave as it evolves under the spherical Burgers equation (1.7) and the boundary conditions (1.6) and (1.8). The parameters ϵ and R_0 are chosen to be 0.01 and 1, respectively. This choice belongs to the domain (S 3) of Scott (see §1). In the initial stage, the evolution is essentially controlled by the inviscid part of (1.7). The numerical and analytic (inviscid) solutions in this regime are found to be

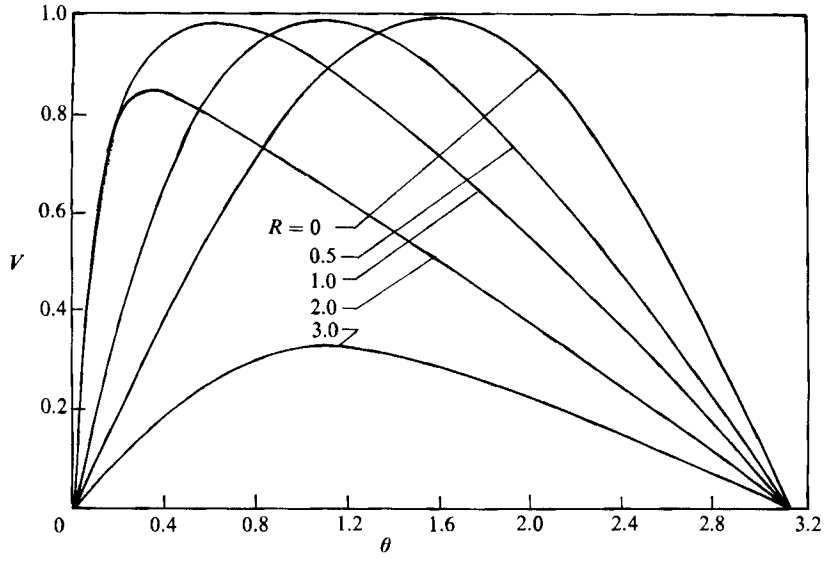

FIGURE 4. Solution of the spherical Burgers equation at $R = 0.5$, 1, 2 and 3 (initial profile at $R = 0$ is also shown).

quite close. For $R > 1$, the wave develops an embryo shock (see figure 4). It may be mentioned here that, as in other geometries, the inviscid solution holds quite accurately to the right of the maximum for $R > 1$. The embryo shock steepens owing to convection until it is resisted by diffusion. Soon the profile acquires a Taylor-shock structure (see figure 4). This regime is followed by a non-quasi-steady shock stage when $R \simeq 4$. The shock broadens and the profile becomes nearly symmetric about $\theta = \frac{1}{2}\pi$ at $R \simeq 5$. At $R = 6$, the profile is strictly symmetric about $\theta = \frac{1}{2}\pi$ and the old-age regime sets in with viscous diffusion and geometry as the only controlling mechanisms.

4. Conclusions

We have carried out a comprehensive numerical investigation of the non-planar Burgers equation (1.1) subject to the boundary conditions (1.2) and (1.8), simulating waves generated by a sinusoidal source. The purpose was first to check some of the asymptotic results of Scott (1981) and Enflo (1985). For this, we first reproduced the analytic results for the planar Burgers equation, which are known via Hopf–Cole transformation. This served several purposes: (i) the regimes over which different analytic solutions – inviscid, Fubini, Fay, and old-age – hold became clearly demarcated; (ii) the canonical nature of the plane problem was re-established with the old-age constant recovered as 4; (iii) the sturdiness and accuracy of the numerical schemes – pseudospectral and implicit predictor–corrector – were confirmed. For most of the domains for non-planar generalized Burgers equations for which Scott (1981) could obtain some analytic results, numerical results were obtained and collated with the analytic ones. In particular, for the canonical problem (3.1) for the cylindrical Burgers equation, treated by Enflo, the old-age constant in (3.1*c*) was computed to be 1.85. This is in reasonable agreement with Enflo's estimate of 2. However, Enflo's analysis needs to be pursued more carefully to dispense with some intuitive arguments. This at the moment seems difficult. The saturation phenomenon

for the cylindrical problem has also been demonstrated (see §3). An interesting feature of the numerical solution is the re-emergence of the symmetry of the solution about $\theta = \frac{1}{2}\pi$ in the old age, albeit the amplitude decreasing exponentially (see (3.2)–(3.7)). The actual numerical solutions are found to agree closely with the analytic old age form, thus providing an excellent check on the veracity of the former in this large time regime.

This work was in part supported by the DST (India) Scheme AM/PLS/129.

REFERENCES

BLACKSTOCK, D. T. 1964 Thermovirus attenuation of plane, periodic, finite-amplitude sound waves. *J. Acoust. Soc. Am.* **36**, 534–542.

COLE, J. D. 1951 On a quasi-linear parabolic equation occurring in aerodynamics. *Q. Appl. Math.* **9**, 225–236.

CRIGHTON, D. G. & SCOTT, J. F. 1979 Asymptotic solutions of model equations in nonlinear acoustics. *Phil Trans. R. Soc. Lond.* A **292**, 101–134.

DOUGLAS, J. & JONES, B. F. 1963 On predictor–corrector methods for nonlinear parabolic differential equations. *J. Soc. Ind. & Appl. Maths* **11**, 195–204.

ENFLO, B. O. 1985 Saturation of a nonlinear cylindric sound wave generated by a sinusoidal source. *J. Acoust. Soc. Am.* **77**, 54–60.

FAY, R. D. 1931 Plane sound waves of finite amplitude. *J. Acoust. Soc. Am.* **3**, 222–241.

FUBINI, E. 1935 Anamolie nella propagazione di onde acustache di grande ampiezza. *Acta Freq.* **4**, 530–581.

LEIBOVICH, S. & SEEBASS, A. R. (eds) 1974 *Nonlinear Waves.* Cornell University Press.

LESSER, M. B. & CRIGHTON, D. G. 1975 Physical acoustics and the method of matched asymptotic expansions. in *Physical Acoustics* (ed. W. P. Mason & R. N. Thurston), vol. 11. Academic Press.

LIGHTHILL, M. J. 1956 Viscosity effects in sound waves of finite amplitude. In *Surveys in Mechanics* (ed. G. K. Batchelor & R. M. Davies). Cambridge University Press.

NAIR, K. R. C. 1988 Numerical and analytic studies of generalised Burgers equations. Ph.D. thesis, Indian Institute of Science, Bangalore, India.

NIMMO, J. J. C. & CRIGHTON, D. G. 1986 Geometrical and diffusive effects in nonlinear acoustic propagation over long ranges. *Phil. Trans. R. Soc. Lond.* A **320**, 1–35.

PARKER, D. F. 1980 The decay of saw-tooth solutions to the Burgers equation. *Proc. R. Soc. Lond.* A **369**, 409–424.

SACHDEV, P. L. 1987 *Nonlinear Diffusive Waves.* Cambridge University Press.

SACHDEV, P. L., TIKĒKAR, V. G. & NAIR, K. R. C. 1986 Evolution and decay of spherical and cylindrical N waves. *J. Fluid Mech.* **172**, 347–371.

SCOTT, J. F. 1981 Uniform asymptotics for spherical and cylindrical nonlinear acoustic waves generated by a sinusoidal source. *Proc. R. Soc. Lond.* A **375**, 211–230.